ISBN: 978-3-95450-219-6 ISSN: 2226-0366 doi: 10.18429/JACoW-LINAC2024-TUPB012

ANOMALOUS FREQUENCY SHIFTS NEAR T_C OF FUNDAMENTAL AND HIGHER-ORDER MODES IN MEDIUM-VELOCITY 644 MHz SUPERCONDUCTING ELLIPTICAL CAVITIES*

S. M. Moskaitis, Y.-L. Cheon, S. Kim, P. N. Ostroumov
Facility for Rare Isotope Beams, Michigan State University, East Lansing, MI, USA

Abstract

Recent studies indicate the magnitude of an anomalous decrease in the resonant frequency, so-called frequency dip, near critical temperature of superconducting niobium cavities, T_c, correlates to the cavity quality factor, Q_0, and impurities introduced into the superconducting niobium surfaces, such as nitrogen or oxygen. We measured frequency dips in both 644 MHz fundamental mode (FM) and 1.45 GHz higher-order mode (HOM) of single-cell elliptical cavities for FRIB energy upgrade (FRIB400) R&D. These measurements were performed in cavities with the following surface treatments: (1) electropolished (EP) only, (2) nitrogen-doped (N-doping), and (3) medium-temperature (mid-T) baked and then hydrofluoric (HF) acid rinsed. We will present measured frequency dips and compare them to cavity Q_0 performance in the FM. Frequency-dependent behavior of frequency dips with various surface treatments will also be discussed as our experimental setup has a unique feature compared to previous studies, which allows for measurement of frequency dips in different modes within the same cavity, in other word, on the same surfaces.

INTRODUCTION

Recent study of bulk superconducting radiofrequency (SRF) niobium cavities has shown a relation between resonant frequency, frequency dip magnitude (denoted $|f_{dip}|$), and anti-Q slope [1].

These relations previously found between resonant frequency, $|f_{dip}|$, and anti-Q slope are of particular interest in the FRIB400 project. This project aims for $Q_0 = 2*10^{10}$ at the accelerating gradient E_{acc} of 17.5 MV/m, operated at 2 K. The study of $|f_{dip}|$ and its cavity-to-cavity behavior could give directions towards producing a 644 MHz 5-cell elliptical cavity for the FRIB400 with lower BCS resistance at the operating E_{acc}, possibly through the realization of anti-Q slope in these 644 MHz cavities, which has not been observed yet in mid-GHz frequency range cavities.

EXPERIMENTAL SETUP

We used three elliptical single-cell niobium SRF cavities in our study. These single-cell cavities have resonant frequencies 644 MHz for their FM and 1.45 GHz for the selected HOM, TM020. These cavities all went through an initial bulk EP, after which the treatment was specific to each cavity. One cavity was nitrogen-doped at 800°C for 2 minutes at 25 mTorr and no annealing under vacuum at 800°C, so-called 2N0 doping, followed by post-doping 5 µm EP. Another cavity was baked at 330°C in the vacuum furnace for 3 hours, followed by a hydrofluoric acid (HF) rinse. The third cavity was simply left with its standard EP as a baseline comparison. These cavities will be referred to as N-doping, mid-T Baking, and baseline EP, respectively.

The dual-mode frequency and temperature measurements of these cavities were performed using the following steps. Lakeshore Cernox-1050 Resistance temperature detectors (RTDs) were placed on the cavity for temperature measurements. The dunk dewar, in which one of the cavities was installed, was initially cooled down and liquid helium was accumulated at 4.5 K. We then pumped down the dewar to 30 – 50 Torr, and started to warm up the cavity at a constant pressure. This is to eliminate the df/dp effect such that the measured frequency is solely a function of temperature. A heater located at the bottom of the dunk dewar was used to control the warm-up speed; we found that once the liquid level was below the cavity assembly, the boil-off of liquid helium enhanced by the heater actually slowed down the cavity warm-up speed. With this technique, we could achieve the warm-up rate slower than 0.05 K/min at around T_c, which was useful to take precise measurement of f_{dip}.

We used two Vector Network Analysers to measure both FM and HOM simultaneously. The FM was amplified up to 3 – 5 W by a 644 MHz amplifier and driven to the cavity through a standard high-power RF transmission line. On the other hand, the HOM was driven via the reflected port of the bi-directional coupler in the RF transmission line. The pickup RF signal was split by a 3-dB splitter and each of them went to the FM/HOM VNA. We could detect almost the same RF power level between FM and HOM because coupling strength of both input and pickup couplers is much higher in the HOM compared to the FM: S21 is approximately 60 dB higher.

For each frequency dataset, the electron mean free path of the cavity surface, l, was found by fitting the experimental data. To do this fitting, the experimental frequency data was converted to penetration depth, $\lambda(T)$, as represented by [2]:

$$\lambda(T) - \lambda(T_0) = \frac{G}{\mu \cdot \pi f^2}\left(f(T) - f(T_0)\right), \qquad (1)$$

*This material is based upon work supported by the U.S. Department of Energy, Office of Science, Office of Nuclear Physics and High Energy Physics and used resources of the FRIB Operations, which is a DOE Office of Science User Facility under Award Number DE-SC0023633 and DE-SC0018362.

ISBN: 978-3-95450-219-6 ISSN: 2226-0366 doi: 10.18429/JACoW-LINAC2024-TUPB012

where G is the cavity geometry factor, μ is the magnetic permeability, f is the measured resonant frequency, T is the measured cavity temperature, and T_0 is a sufficiently low temperature ($T < 5$ K) such that the frequency at this temperature is representative of the frequency at 0 K. This penetration depth data was then fit to theoretical data calculated using a code written by Halbritter called SRIMP [3].

DISCUSSION OF RESULTS

There was a notable dip in frequency of both measured modes just below T_c for two of the three FRIB cavities, shown in Fig. 1(a) and 1(b). Table 1 lists these frequency dip magnitudes, $|f_{dip}|$, with the fitted mean free paths of each cavity. The $|f_{dip}|$ values increase in the cavity order of baseline EP, N-Doping, and then mid-T Baking. This trend of increasing $|f_{dip}|$ with decreasing mean free path has been seen in a previous study at FNAL on 1.3 GHz cavities [1].

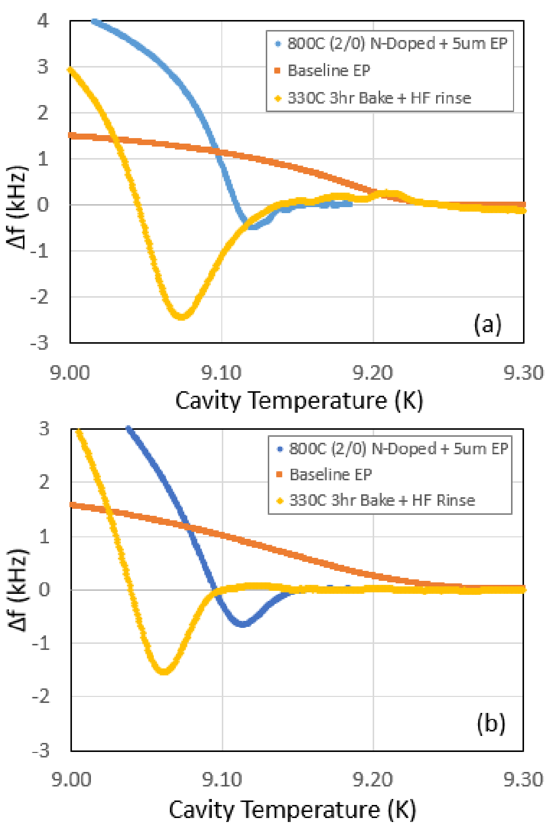

Figure 1: Frequency shifts relative to the normal-conducting state of (a) the FM, TM010, and (b) an HOM, TM020, in 3 Nb SRF cavities with various surface treatments.

Table 1: Frequency Dip Magnitudes

Cavity Treatment	l (nm)	$\lvert f_{dip}^{FM}\rvert$ (kHz)	$\lvert f_{dip}^{HOM}\rvert$ (kHz)
Baseline EP	323 ± 80	0 ± 0.10	0 ± 0.05
N-Doping	40 ± 9	0.53 ± 0.10	0.67 ± 0.05
mid-T Baking	26 ± 7	2.65 ± 0.80	1.65 ± 0.10

The mean free paths in Table 1 were fitted from the measured frequency shifts, which were then converted to penetration depth changes using Eq. (1) in the temperature range of 6.0 K to near T_c. Particularly in the N-doping case, we found the mean free path of our 2N0 + 5 µm post EP cavity is roughly consistent with the previous study in 1.3 GHz performed by Cornell [4].

An important detail in this consistency check was the difference in doping and annealing time between our 800°C 2N0 N-Doping case and Cornell's 800°C 30N20 N-Doping. The amount of EP, denoted as depth, was normalized to remove the dependence of the combined doping and annealing time on the mean free path. This normalization was carried out using

$$x_{\text{norm}} = x_{\text{exp}}\sqrt{\frac{t_{\text{norm}}}{t_{\text{exp}}}}\ , \qquad (2)$$

an equation formed using doping relations from [5]. In Eq. (2), t_{exp} is our cavity's combined doping time of 2 minutes, x_{exp} is the 5 µm post-doping EP on our cavity, and t_{norm} is the combined doping and annealing time the cavity is being normalized to, which in this case is the 50 minutes of Cornell's 30N20 N-Doping. This gives an x_{norm}, normalized depth, of 25 µm for our N-Doping case, which was used in the consistency check between our case and Cornell's.

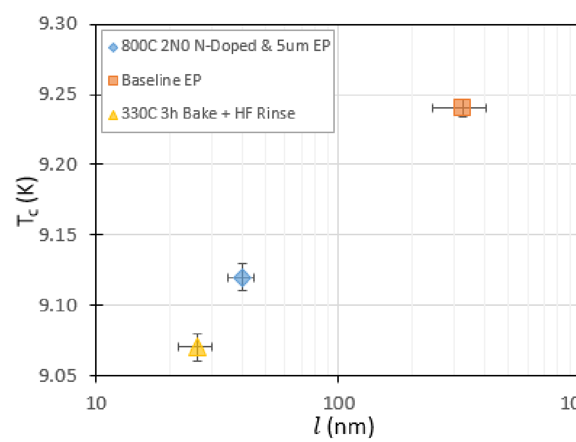

Figure 2: T_c plotted against SRIMP fitted l for the three 644 MHz FRIB Nb cavities of varying surface treatment.

We found that increased impurity concentration of nitrogen or oxygen (shorter mean free path) resulted in a decrease in T_c, as shown in Fig. 2 and reported in the previous study [1]. The trend of T_c decreases with the mean free path in our cases, regardless of N-doping or mid-T baking, is aligned with what Fermi measured in 1.3 GHz N-doped cavities [1].

In order to compare frequency dips measured in two different modes, we introduce a normalized frequency dip $|f_{\text{dip,norm}}|$, as defined by

$$|f_{\text{dip,norm}}| = \left(\frac{G}{G_{\text{norm}}}\right)\left(\frac{f_{\text{norm}}}{f}\right)|f_{\text{dip}}|\ ,$$

ISBN: 978-3-95450-219-6 ISSN: 2226-0366 doi: 10.18429/JACoW-LINAC2024-TUPB012

where f is the resonance frequency and G is the geometric factor of each mode. We used f_{norm} of 1.3 GHz and G_{norm} of 270 Ohm as normalization parameters chosen from the 1.3 GHz TESLA cavity for easier comparison with the previous studies [1,6].

Table 2: Normalized Frequency Dip Magnitudes

Cavity Treatment	$\lvert f_{dip,norm}^{FM} \rvert$ (kHz)	$\lvert f_{dip,norm}^{HOM} \rvert$ (kHz)
Baseline EP	0 ± 0.15	0 ± 0.08
N-Doping	0.77 ± 0.15	1.05 ± 0.08
mid-T Baking	3.83 ± 1.16	2.58 ± 0.16

We found that the $\lvert f_{\mathrm{dip,norm}} \rvert$ was similar between modes in the N-doping case, but less so between the modes in the mid-T Baking case, as seen in Table 2. This similarity in the N-Doping case is particularly interesting as we did not observe anti-Q slope in our FM 2 K Q-curve, while the 1.3 GHz TESLA cavities had apparent anti-Q slopes even with greater mean free paths than our N-Doping case [1,7]. The variation in modal $\lvert f_{\mathrm{dip,norm}} \rvert$ difference between the N-Doping and mid-T Baking cases and lack of anti-Q slope observation in our FM 2 K Q-curve suggests further studies of 1.45 GHz HOM 2 K Q-curve measurements in our cavities as well as dual-mode frequency dip measurements at additional mean free paths with different doping recipes.

CONCLUSION

We conducted dual-mode frequency measurements of cavities near T_c. Frequency was then converted to penetration depth, fitted to determine mean free path, and then these mean free paths were validated. Also, positive correlations were found between mean free path and $\lvert f_{\mathrm{dip}} \rvert$ as well as T_c and mean free path, which agreed with a previous FNAL study [1]. In addition, we found that modal $\lvert f_{\mathrm{dip,norm}} \rvert$ differences vary between our N-Doping and mid-T Baking cases along with a lack of observed anti-Q slope in our FM 2 K Q-curve, which both suggest the need of additional study.

ACKNOWLEDGEMENTS

The Authors appreciate supports for SRF cavity surface processing, cavity assembly, experimental setup for dunk tests, cryogenic operations from FRIB SRF and Cryogenics groups.

REFERENCES

[1] D. Bafia, M. Checchin, A. Grassellino, A. Romanenko, and J. Zasadzinski, “Investigating the Anomalous Frequency Variations Near Tc of Nb SRF Cavities”, in *Proc. SRF'21*, East Lansing, MI, USA, Jun. 2021, p. 885. doi:10.18429/JACoW-SRF2021-FROFDV03

[2] J. Halbritter, “Change of eigenstate in a superconducting RF cavity due to a nonlinear response”, *Journal of Applied Physics,* vol. 41, no. 11, pp. 4581–4588, 1970. doi:10.1063/1.1658500

[3] J. Halbritter, “FORTRAN-Program for the Computation of the Surface Impedance of Superconductors”, *Institut fuer Experimentelle Kernphysik (IEKP),* Rep. KFK-Ext 03/70-06, 1970. doi:10.5445/IR/270004230

[4] D. Gonnella, “The fundamental science of nitrogen-doping of niobium superconducting cavities”, Ph.D. thesis, Phys. Dept., Cornell University, Ithaca, New York, 2016.

[5] J. Clenny and C. Rosa., “Nitridation kinetics of niobium in the temperature range of 873 to 1273 K”, *Metallurgical Transactions A*, vol. 11, pp. 1575–1580, Sept. 1980. doi:10.1007/BF02654521

[6] B. Aune *et al.*, “Superconducting TESLA cavities”, *Phys. Rev. ST Accel. Beams,* vol. 3, p. 092001, Sept. 2000. doi:10.1103/PhysRevSTAB.3.092001

[7] K. McGee *et al.*, "Advanced surface treatments for medium-velocity superconducting cavities for high-accelerating gradient continuous-wave operation", *Nuclear Instruments and Methods in Physics Research Section A: Accelerators, Spectrometers, Detectors and Associated Equipment*, vol. 1059, p. 168985, Feb. 2024. doi:10.1016/j.nima.2023.168985